Theoretical and experimental study of the chemisorption of 1,3 disilabutane on the Si(100) surface

ARTICLE *in* THE JOURNAL OF CHEMICAL PHYSICS · MARCH 2003

Impact Factor: 2.95 · DOI: 10.1063/1.1544092

Theoretical and experimental study of the chemisorption of 1,3 disilabutane on the Si(100) surface

G. Valente,[a] C. R. Stoldt, R. Maboudian,[b] and C. Carraro
Department of Chemical Engineering, University of California, Berkeley, California 94720

(Received 17 June 2002; accepted 12 December 2002)

The adsorption of 1,3 disilabutane on Si(100)-(2×1) is studied both computationally and experimentally. First, the possible adsorption species are calculated through density functional theory using the Becke three parameter Lee–Yang–Parr functional. The Si_9H_{12} cluster is adopted to simulate the Si(100) dimer. Frequency calculations are also performed to find the harmonic frequencies and infrared intensities of the calculated species. Adsorption experiments are then performed on the Si(100)-(2×1) surface. The surface is subsequently characterized using high-resolution electron energy loss spectroscopy. By comparing calculated and experimental spectra, it is found that the most probable adsorption product is the $C_2H_9Si_2$ species bonded to the surface through a silicon–silicon bond. To confirm this finding, the transition state of this reaction is calculated and compared with other possible adsorption paths. It is found that the chemisorption reaction leading to silicon–silicon bonded $C_2H_9Si_2$ is the most probable reaction with an activation energy of about 11 kcal/mol. © *2003 American Institute of Physics.* [DOI: 10.1063/1.1544092]

I. INTRODUCTION

Silicon carbide (SiC) is receiving increasing attention as an interesting material in both microelectronics and micro electro-mechanical system (MEMS) technologies. As a semiconductor, its large energy bandgap (ranging from 2.4 to 3.1 eV) and large electronic saturation velocity (about 2×10^7 cm/s) permit high-frequency, high-power operation;[1] as a ceramic, its Young modulus (700 GPa), high hardness and excellent resistance to wear and to chemical attack[2] make it an ideal material for micro- and nanomechanical applications.[3]

Another attractive characteristic of silicon carbide is that it can be grown on silicon substrates to obtain either epitaxial or polycrystalline films by chemical vapor deposition, thus permitting integration with silicon microfabrication technology. Different processes are reported in the literature depending on the adopted precursor; the most widely adopted process is based on feeding silane and propane diluted in hydrogen in a chemical vapor deposition reactor at atmospheric pressure. Under these conditions, polycrystalline films are obtained at temperatures in excess of 1000 °C,[4] while epitaxial films are obtained at 1400 °C.[5] These elevated temperatures are not compatible with standard silicon microfabrication processes. More recently, efforts have addressed the use of single-source precursors in chemical vapor deposition, where the precursor molecule contains both silicon and carbon atoms.[2,6,7] In this process, the deposition temperature can be kept substantially lower than in the $SiH_4-C_3H_8$ process and the additional step of surface precarbonization is not required. In particular, 1,3 disilabutane, $SiH_3-CH_2-SiH_2-CH_3$ (1,3-DSB) has been demonstrated to be a very promising single precursor. Boo *et al.*[6] were able to grow epitaxial SiC at temperatures ranging between 900 and 1000 °C, while polycrystalline silicon carbide was obtained at 700 °C.

In spite of its great promise, this process is relatively new and, from a fundamental point of view, largely uncharacterized. It is clear that the kinetics of precursor adsorption and the surface processes at the initial stages of growth play an important role in facilitating heteroepitaxial growth and determining the morphology of the film. However, to our knowledge, only one experiment has been reported that focused on the chemisorption kinetics of 1,3-DSB on Si(111). Park *et al.*[8] performed Cs^+ reactive ion scattering and secondary ion mass spectroscopy to identify the adsorption product on the Si(111)-(7×7) surface. They found that the 1,3-DSB reacts with the silicon surface to give $C_2H_8Si_2$ and CH_4Si adsorbed species in the temperature range from 150 to 270 K. No studies are reported on the adsorption of 1,3-DSB on Si(100). The temperature difference between the surface science studies and the process conditions is such that some activated processes do not take place in the surface science experiments, so that only low activation energy processes are seen when performing experiments at low temperature. This allows the isolation of the first adsorption step, but other highly activated processes, which take place during the CVD growth, are not seen in these experiments.

The aim of the present work is to obtain quantitative information about the adsorbed species on the Si(100) surface by means of quantum-chemical computations and high-resolution electron energy loss spectroscopy. We find that the most probable reaction pathway produces silicon bonded species. In particular, the lowest activation energy corresponds to the breaking of the Si–H bond in the 1,3-DSB giving adsorbed $C_2H_9Si_2$, which can react again on the surface to give adsorbed $CH_3-SiH-CH_2-SiH_2$. The calculated

[a]On leave from: Dipartimento di Materiali, Chimica e Ingegneria Chimica "Giulio Natta," Politecnico di Milano, Via Mancinelli 7, 20131 Milano.
[b]Electronic mail: maboudia@socrates.berkeley.edu

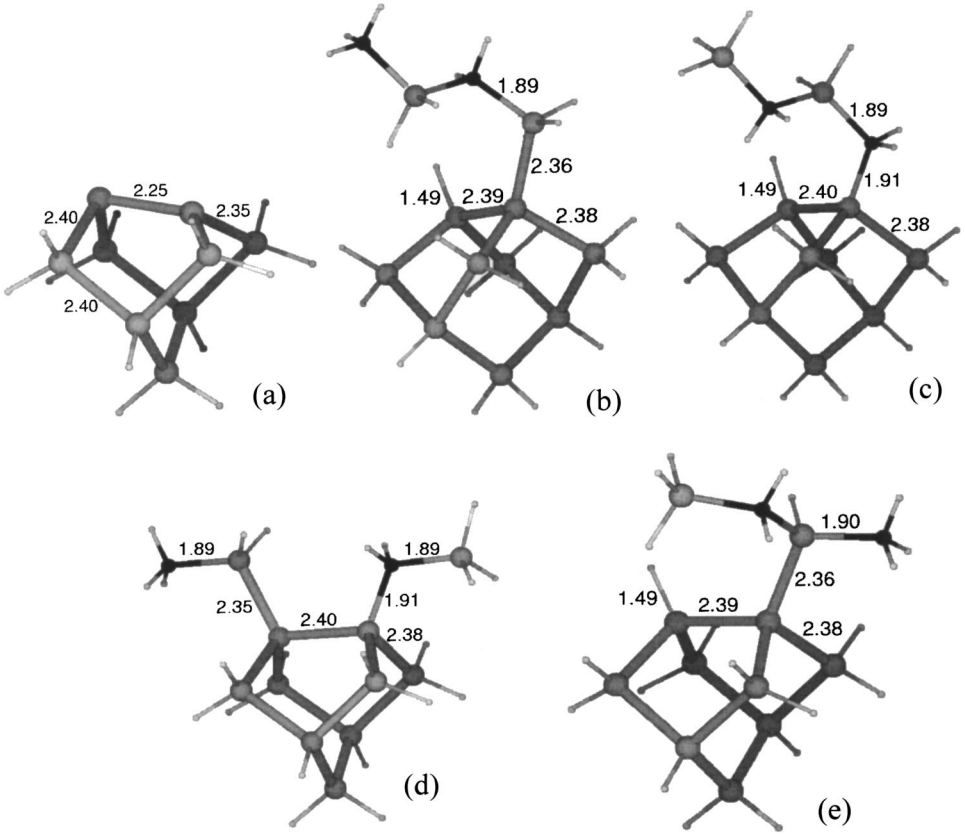

FIG. 1. Calculations performed with the Si_9H_{12} cluster: (a) cluster, (b) 1-Si bonded $C_2H_9Si_2$, (c) C-bonded $C_2H_9Si_2$, (d) $CH_3SiH_2^* + CH_2SiH_3^*$, (e) 3-Si bonded $C_2H_9Si_2$. Black spheres correspond to C and small spheres to H.

activation energies for these two processes are determined to be 11.6 and 14.3 kcal/mol, respectively.

II. THEORETICAL AND COMPUTATIONAL METHODS

Following established practices,[9–13] the Si(100) surface is modeled using the Si_9H_{12} cluster, represented in Fig. 1(a). Some geometries are also calculated with the $Si_{15}H_{16}$ cluster, represented in Fig. 2(a), to check for cluster size effects. The two clusters are designed to represent one and two silicon dimers, respectively; all unpaired electrons of the silicon atoms are saturated with hydrogen atoms. Configurations are optimized using density-functional theory (DFT) with the B3LYP[14] hybrid functional to calculate exchange and corre-

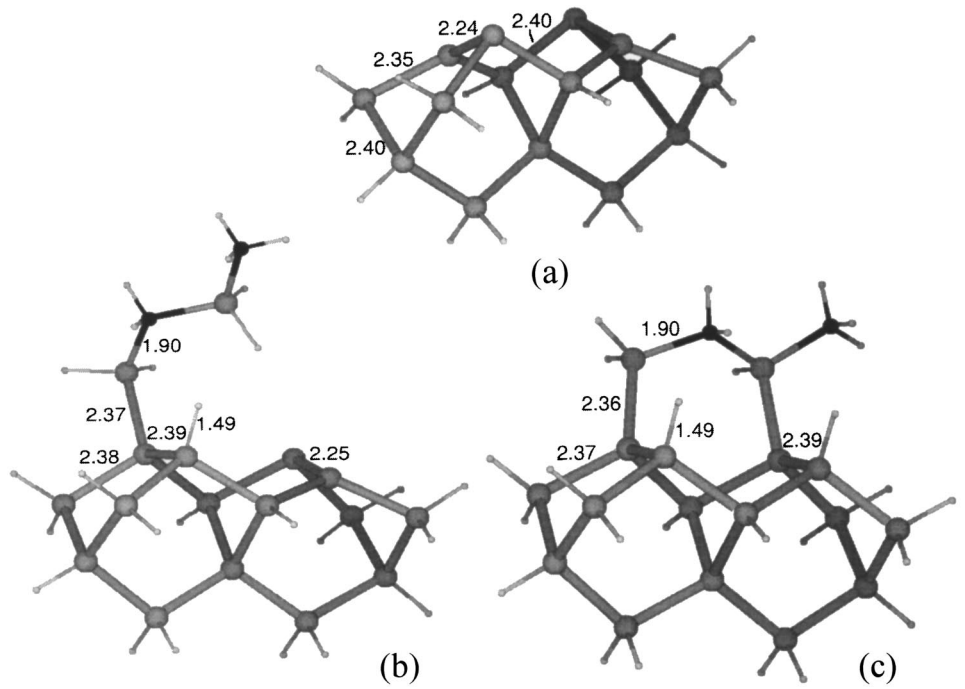

FIG. 2. Calculations performed with the $Si_{15}H_{16}$ cluster. (a) cluster, (b) adsorbed $C_2H_9Si_2$, (c) adsorbed $CH_3-SiH-CH_2-SiH_2$. Black spheres correspond to C and small spheres to H.

lation energies; all calculations are performed using GAUSSIAN 98.[15] Different basis sets are chosen depending on the position of the atoms: for the top atoms, representing the surface silicon dimers, the 6-31G(d,p) basis set is adopted, while for all other Si atoms of the cluster, a 6-31G basis set without polarization functions is used. The hydrogen atoms, which saturate the unpaired electrons, are described with the sto-3G basis set. This approach allows a reduction in the computational time by reducing the basis set for the cluster atoms, which are not involved in the reaction. A similar approach was adopted by Raghavachari *et al.*[9] with the second-order Moller–Plesset (MP2) method. In this work the basis set is also strongly reduced for the hydrogen atoms terminating the unsaturated electrons of the cluster. The geometries of all species are optimized without any constraints and a frequency calculation is performed for each species. All calculated frequencies are positive.[16] Transition states are checked with a frequency calculation, to verify that only one imaginary frequency exists for every transition state. Further, the imaginary frequency is analyzed by inspection to make sure that it does not correspond to internal rotations.

To facilitate the comparison of the calculated vibrational spectra with experimental HREEL spectra, the frequency calculations are performed after endowing all ''spectator'' atoms with a fictitious atomic weight of about 1000 g/mol. We consider spectator atoms to be all hydrogen atoms that saturate the unphysical dangling bonds of the silicon cluster, as well as the bulk Si atoms, i.e., those not belonging to the DSB molecule or to a surface dimer. With this approach, all the frequencies related to the motion of the cluster are lowered, leaving only the frequencies of the dimer and the adsorbate in the range between 200 and 4000 cm^{-1}. It is checked that this procedure does not significantly affect the frequencies of the adsorbed molecule. The check is performed on silicon bonded $C_2H_9Si_2^*$ as follows: First, a frequency calculation is performed with the real atomic weight for each atom, then the same frequency calculation is repeated after increasing the weight of the spectator atoms. By comparing the two calculations, it is found that the procedure does not affect the harmonic frequencies related to the adsorbate, the only noticeable effect being the lowering of the Si–H frequencies related to the cluster. Frequencies calculated in this manner are then corrected with a scaling factor of 0.9613, as indicated by Scott and Radom.[17]

The adsorption enthalpies are calculated as the difference between products and reactants enthalpies; enthalpies of each species are calculated as the sum of the electronic energy, zero-point correction and thermal correction. Activation energies, instead, are calculated as the difference between transition state energies and reactant energies, zero-point corrected.

III. COMPUTATIONAL RESULTS ON SELECTED ADSORPTION REACTIONS

Five species are calculated as the possible adsorption products. The first two species are represented in Figs. 1(b) and 1(c), and correspond to the silicon-bonded and the carbon-bonded $C_2H_9Si_2^*$ in position 1, respectively. The ''star'' after the chemical formula denotes a surface species. It is important to note that these species have a vertical configuration. The corresponding adsorption reactions are

$$CH_3-SiH_2-CH_2-SiH_3+Si{=}Si \rightarrow CH_3-SiH_2-CH_2-SiH_2-Si-Si-H, \quad (R1)$$

$$CH_3-SiH_2-CH_2-SiH_3+Si{=}Si \rightarrow SiH_3-CH_2-SiH_2-CH_2-Si-Si-H, \quad (R2)$$

where Si═Si denotes the silicon surface dimer and $CH_3-SiH_2-CH_2-SiH_2-Si-Si-H$ and $SiH_3-CH_2-SiH_2-CH_2-Si-Si-H$ correspond to the species represented in Figs. 1(b) and 1(c), respectively.

The enthalpies for reactions (R1) and (R2) are −52.4 and −46.5 kcal/mol, respectively, thus showing that reaction (R1) is energetically favored with respect to reaction (R2). Transition states were also found for both reactions: Reaction (R1) has activation energy $E_a=11.6$ kcal/mol, while reaction (R2) has activation energy $E_a=30.7$ kcal/mol. It is worthwhile to note that the barrier of reaction (R1) is very similar to the calculated adsorption barrier for silane on Si(100), recently calculated by Kang and Musgrave.[18] They found a value of 11.3 kcal/mol, using a Si_9H_{12} cluster and B3LYP method with 6-311++G($2pd$,$2df$) basis set.

Next, the dissociative adsorption of 1,3-DSB is considered by breaking of the central Si–C bond, according to reaction

$$CH_3-SiH_2-CH_2-SiH_3+Si{=}Si \rightarrow CH_3-SiH_2-Si-Si-CH_2-SiH_3. \quad (R3)$$

Species $CH_3-SiH_2-Si-Si-CH_2-SiH_3$ is shown in Fig. 1(d) and it may be considered as two surface species: $CH_3-SiH_2^*$ and $SiH_3-CH_2^*$. For this reaction, the calculated adsorption enthalpy is −50.7 kcal/mol, while the transition-state calculation predicts an activation energy of 33.9 kcal/mol. The comparison between reactions (R1)–(R3) shows that formation of the silicon–silicon bond by breaking of the silicon-hydrogen bond is the most energetically *and* kinetically favored process.

In addition, a calculation is performed for adsorption by means of the breaking of the silicon-hydrogen bond in position 3, i.e., through the reaction

$$CH_3-SiH_2-CH_2-SiH_3+Si{=}Si \rightarrow CH_3-\underset{\substack{|\\ Si-SiH}}{SiH}-CH_2-SiH_3 \quad (R\text{-}1bis)$$

The adsorbed species is still a silicon-bonded $C_2H_9Si_2^*$ but the surface dimer is bonded to the third silicon atom of the 1,3-DSB chain. This species is represented in Fig. 1(e). The calculated adsorption enthalpy is −51.6 kcal/mol, while transition state calculation predicts an activation energy of 9.2 kcal/mol. The values of adsorption enthalpy and activation energy for this case are very similar to those found for reaction (R1).

Another calculated species is $CH_3-SiH-CH_2-SiH_2^*$ which, according to Park *et al.*,[8] is the adsorption product on the Si(111) surface. In this case, the adsorbed species is horizontally oriented on the surface, bridging two Si atoms from

TABLE I. Adsorption energies for the calculated species and activation energies for the corresponding adsorption reaction.

Adsorbed species	Adsorption enthalpy (kcal/mol)	Adsorption activation energy (kcal/mol)
1-Si bonded $C_2H_9Si_2$	−52.4	11.6
$C_2H_9Si_2$ C bonded	−46.5	30.7
$CH_3SiH_2^* + CH_2SiH_3^*$	−50.7	33.9
3-Si bonded $C_2H_9Si_2$	−51.6	9.2
$C_2H_9Si_2$ Si bonded (on $Si_{15}H_{16}$)	−48.5	···
$CH_3-SiH-CH_2-SiH_2$ Si bonded (on $Si_{15}H_{16}$)	−102.4	14.3

two adjacent dimers. The $Si_{15}H_{16}$ cluster [Fig. 2(a)] is adopted to simulate this species on the Si(100) surface, because the bonding now involves two surface dimers. The geometry of the $CH_3-SiH-CH_2-SiH_2^*$ species is shown in Fig. 2(c) and for comparison, the 1-Si bonded $C_2H_9Si_2^*$ species is shown in Fig. 2(b). Other configurations for the adsorbed molecules may exist in principle, but the configuration examined here is chosen according to the fact that the silicon–silicon bond formation is the most favored process. The adsorption enthalpy is calculated according to reactions (R4) and estimated to be −102.4 kcal/mol,

$$\begin{aligned} &CH_3-SiH_2-CH_2-SiH_3 + Si{=}{=}Si \\ &\quad \rightarrow CH_3-SiH-CH_2-SiH_2 + 2H^* \\ &\qquad\quad\ \ |\qquad\quad\ \ | \\ &\qquad\quad Si\qquad\ \ Si. \end{aligned} \tag{R4}$$

The horizontally oriented species has two bonds with the surface but a concerted process in which the two bonds react simultaneously is statistically excluded; i.e., it is thought that the probability that the molecule impacts in the right position to permit a simultaneous reaction of silicon atom in position 1 and in position 3 is low with respect to the probability that other processes occur. Moreover, 1,3-DSB does not possess any double bonds that might lead to concerted processes like Deals–Alder reactions. Thus, reaction (R4) is thought to occur via two steps: In the first step, gas phase 1,3-DSB reacts with the surface to give the $C_2H_9Si_2^*$ species, while in the second step, adsorbed $C_2H_9Si_2^*$ reacts with another dimer to give $CH_3-SiH-CH_2-SiH_2^*$. If $C_2H_9Si_2^*$ adsorption occurs first through reaction (R1), then $CH_3-SiH-CH_2-SiH_2^*$ can be obtained through reaction (R5):

$$\begin{aligned} &CH_3-SiH_2-CH_2-SiH_2-Si-Si-H + Si{=}{=}Si \\ &\quad \rightarrow CH_3-SiH-CH_2-SiH_2 + H^* \\ &\qquad\quad\ \ |\qquad\quad\ \ | \\ &\qquad\quad Si\qquad\ \ Si. \end{aligned} \tag{R5}$$

The transition state for reaction (R5) has been calculated, yielding an activation energy of 14.3 kcal/mol. All the adsorption energies and the activation energies (where available) are summarized in Table I.

IV. EXPERIMENT

The 1,3-DSB adsorption experiments are performed in an ultrahigh vacuum chamber with base pressure below 2×10^{-10} Torr. The Si(100) samples are first etched in concentrated HF, then rinsed in acetone and introduced into the vacuum chamber via a load lock. Before 1,3-DSB exposure, the samples are annealed to ~1000 °C for 10 seconds. The low-energy electron diffraction pattern confirmed that this procedure yields the (2×1) surface reconstruction. The 1,3-DSB precursor was obtained from Gelest Inc. with purity greater than 96%. The DSB exposure is given in units of Langmuir, where 1 Langmuir (L)$=10^{-6}$ Torr·s. HREEL spectra are obtained with a LK Technologies model ELS3000 spectrometer, using an incident electron energy of 7 eV at an incident angle of 60° toward the surface normal. All the adsorption experiments reported here are carried out at room temperature. The sample temperature was held at about 100 K during HREEL spectra acquisition.

Raman and IR spectra are obtained from liquid 1,3-DSB, using a Hololab Series 5000 Research Raman spectrometer with a laser wavelength of 532 nm and a Mattson Infinity 60 MI Fourier-transform infrared (FTIR) spectrometer, respectively.

V. DISCUSSION OF THE SPECTRA

A. Liquid 1,3-DSB

To check the reliability of the quantum chemical frequency calculation for the Si–C–H system, the Raman and IR spectra of liquid DSB are compared to the calculated spectra.[19] Optimization and frequency calculation of 1,3-DSB are performed both by density functional theory (B3LYP method, as described previously) and by MP2(FC) method. In both cases, the 6-31G(d,p) basis set is adopted. Figure 3(a) shows calculated and experimental Raman spectra, while Fig. 3(b) shows calculated and experimental IR spectra. The assignment of the vibrational modes (based on literature and on the analysis of the displacement eigenvectors) is shown in Table II. The Raman frequencies are about 15 cm^{-1} higher than the IR frequencies, most likely due to systematic experimental error. The calculated frequencies are for the most part in agreement with experimental data to within about 20 cm^{-1}, with the exception of the CH stretching modes that are overestimated by up to 40 cm^{-1} by the B3LYP method and by up to 60 cm^{-1} by the MP2 method. The calculated low frequencies are generally in good agree-

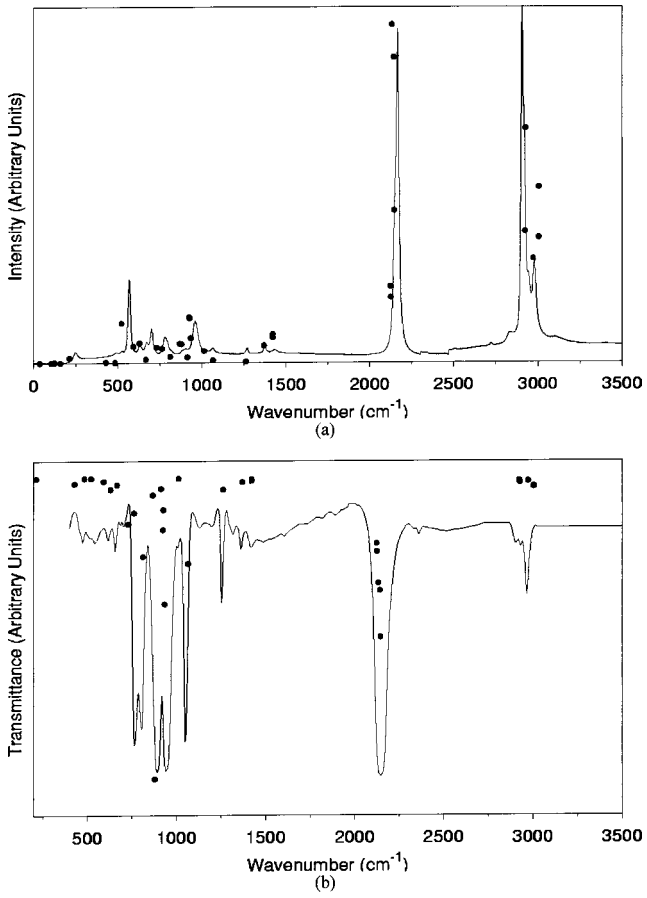

FIG. 3. Raman (a) and IR (b) spectra of liquid 1,3-DSB. The symbols ● display the calculated frequencies through B3LYP method. Vertical positions of the points are a scaled intensity of the calculated intensity.

ment with the IR spectrum, while high frequencies seem to be in better agreement with the Raman spectra. Particularly important modes for the analysis to follow are the SiH stretching at 2170 cm^{-1}, the CH_3 deformation modes at 1420 and 1260 cm^{-1} and the SiH_2 wag at 892 cm^{-1}.

B. Adsorbed 1,3-DSB

The HREEL spectrum, following a 0.5 L exposure of 1,3-DSB at 300 K, is shown in Fig. 4. This exposure is approximately equal to the saturation exposure reported by Okada *et al.*[21] for 1,4 disilabutane on Si(100)-(2×1) substrate. The fact that even at such a low exposure it is possible to obtain adsorption is indicative of the high reactivity of the DSB on the silicon surface.

The CH stretching modes in the region between 2930 and 3000 cm^{-1}, the SiH stretching modes near 2100 cm^{-1}, two peaks at 1250 and 1370 cm^{-1} are readily identified. A very intense peak can be identified at 800 cm^{-1} and two shoulders can be found at 880 cm^{-1} and at 1030 cm^{-1}, respectively. Smaller peaks can be identified at 624 and 470 cm^{-1}. The assignment of the frequencies according to literature data is reported in Table III.

The shift in the maximum intensity of the SiH stretching from 2170 cm^{-1} in the liquid to 2090 cm^{-1} in the HREEL spectrum suggests that 1,3-DSB chemisorbs on silicon; in fact, according to Imbhil *et al.*[22] and to Tautz and Schaefer,[23] the observed 2090 cm^{-1} frequency can be attributed to SiH_2 and SiH stretch but not to SiH_3 stretch, which is blue-shifted to 2140 cm^{-1}.[21,22,24] *This observation indicates that the majority of the* SiH_3 *groups are broken and that 1,3-DSB is predominantly silicon bonded*. Further confirmation of Si bonding is provided by the presence of the CH_3 stretching at 2980 cm^{-1} and of the CH_3 degenerate and symmetric deformation modes at 1410 and 1237 cm^{-1}, respectively, indicating that, unlike SiH_3, the CH_3 group is predominantly intact after chemisorption.

This interpretation of the HREEL spectra is further supported by the DFT frequency calculations performed with B3LYP method. The frequencies of the calculated species are presented in Table IV. Five species are reported: Carbon-bonded $C_2H_9Si_2^*$, silicon-bonded $C_2H_9Si_2^*$ through silicon in position 1 (referred as 1-Si bonded $C_2H_9Si_2^*$), silicon-bonded $C_2H_9Si_2^*$ through silicon in position 3 (3-Si bonded $C_2H_9Si_2^*$), the species resulting from the Si–C bond breakage (referred as $CH_3-SiH_2^*$ and $SiH_3-CH_2^*$) and the bridge silicon-bonded $CH_3-SiH-CH_2-SiH_2^*$. The best agreement between experimental spectrum and calculated frequencies is obtained for the 1-Si bonded $C_2H_9Si_2^*$, as described next.

For the carbon-bonded species, the higher CH_3 asymmetric stretching frequency, experimentally observed around 3000 cm^{-1}, is not present in the calculation while the highest calculated SiH stretching (corresponding to SiH_3) at 2150 cm^{-1}, is not present in the experiment. In contrast, for the 1-Si bonded $C_2H_9Si_2^*$ and the $CH_3-SiH-CH_2-SiH_2^*$ species, the CH_3 asymmetric stretching frequencies are calculated at 3006 and 3009 cm^{-1}, respectively. Furthermore, the highest SiH stretching modes are assigned to the SiH_2 stretching and are red-shifted down to 2129 and 2120 cm^{-1}, respectively. The broken DSB indicated as $CH_3SiH_2^* + CH_2SiH_3^*$ and the 3-Si bonded $C_2H_9Si_2^*$ have characteristics similar to the carbon-bonded $C_2H_9Si_2^*$ because of the presence of the SiH_3 group. Furthermore, for the carbon-bonded species, the frequency calculation shows that the 1261 and 1418 cm^{-1} modes, seen experimentally, disappear. According to the calculation, these modes are related to the CH_3 symmetric and asymmetric deformations; this is also in agreement with experimental data of CH_3SiH_3 taken from Shimanouci.[25] A close-up of these peaks is shown in Fig. 5. The 1237 cm^{-1} peak in the spectrum is overestimated by the calculation while the broader peak at 1380 cm^{-1} can be assigned to the 1365 and 1418 cm^{-1} modes.

In the region between 800 and 1100 cm^{-1}, three modes can be identified from the HREEL spectrum at 800, 880, and 1030 cm^{-1} with the 800 cm^{-1} mode particularly strong. From frequency calculations of the 1-Si bonded $C_2H_9Si_2^*$, we found two very strong IR modes at 817 and 884 cm^{-1}. Both modes are related to SiH_2 wag. The first mode (at 817 cm^{-1}) corresponds to the wag mode of the SiH_2 group bonded to the silicon surface. In this mode, the oscillation is in the direction normal to the surface. This mode is excited primarily by dipole scattering according to the dipole selection rule[26] and because the predicted IR intensity is very strong, then the HREELS intensity is also expected to be very strong. The other mode corresponds to an oscillation of the SiH_2 group farther from the surface and with smaller

TABLE II. Assignment of the molecular frequencies of 1,3-DSB.

IR peak (cm^{-1})	Raman peak (cm^{-1})	Calculated peak (b31YP) (cm^{-1})	Calculated peak (MP2) (cm^{-1})	Vibrational modes (calculated)	Literature frequency (cm^{-1})	Molecule [Ref.]
2966	2982	3005	3029	CH_3 d-str	2982	CH_3SiH_3[a]
2932	2920	2972	2992	CH_2 a-str	2930	n-C_4H_{10}[b]
2907	2910	2927	2933	CH_3 s-str	2898	CH_3SiH_3[a]
		2922	2931	CH_2 s-str	2887	n-C_3H_8[b]
					2853	n-C_4H_{10}[b]
2151	2169	2145	2180	SiH_3 str	2160	1,4-DSB[c]
		2142	2177			
		2132	2170			
		2125	2158	SiH_2 str		
		2123	2156			
1420	1433	1421	1421	CH_3 d-deform	1403	CH_3SiH_3[a]
1362	1377	1369	1364	CH_2 bend	1462	n-C_3H_8[b]
					1410	1,4-DSB[c]
					1382	CH_2Br_2[b]
1256	1271	1263	1271	CH_3 s-deform	1260	CH_3SiH_3[a]
1051	1066	1065	1070	CH_2 wag	1195	CH_2Br_2[b]
					1064	1,4-DSB[c]
942	961	934	954	SiH_2 bend	954	SiH_2Cl_2[b]
···	···	924	944	SiH3 d-deform	927	1,4-DSB[c,d]
···	···	914	930	SiH3 s-deform	919	1,4-DSB[c,d]
892	···	878	885	SiH_2 wag	876	SiH_2Cl_2[b]
803	···	812	817	CH_2 rock $-SiH_2$ twist	···	···
766	782	763	767	CH_3 rock $-SiH_2$ wag	···	···
···	701	730	737	Si–C str	700	CH_3SiH_3[a]
658	673	667	675	Si–C str	···	···
617	633			[e]	···	···
		629	632			
542	569	593	587	[e]	···	···

[a]Reference 25.
[b]T. Shimanouchi, Tables of Molecular Vibrational Frequencies Consolidated Volume I, National Bureau of Standards, 1–160 (1972).
[c]Reference 24.
[d]The authors of Ref. 24 call these modes generically as HSiH bend.
[e]These frequencies were not described with the usual names because of the difficult is in identifying a clear movement of the molecule.

normal component, resulting in an electron energy loss mode of lower intensity.

In the $CH_3-SiH-CH_2-SiH_2^*$ silicon-bonded species, only one SiH_2 wag mode is found at 840 cm^{-1}; other IR intense modes for $CH_3-SiH-CH_2-SiH_2^*$ can be found at 878 and 911 cm^{-1} corresponding to the SiH_2 bend and to the CH_3 rock respectively, but these vibrational modes have small components perpendicular to the surface and, thus, they are not expected to be very intense in a HREEL spectrum.[26]

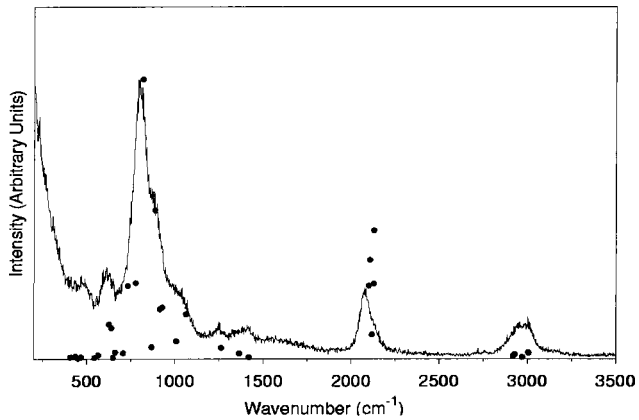

FIG. 4. HREEL spectrum of adsorbed 1,3-DSB for 0.5L exposure (solid line) and calculated frequencies and IR intensities for Si-bonded $C_2H_9Si_2$ (●).

These considerations confirm collectively that the adsorption products are predominantly silicon bonded. A particularly good agreement is found between experiments and the calculated spectrum of the vertically oriented, 1-Si bonded $C_2H_9Si_2^*$, although one cannot exclude the presence of horizontal $CH_3-SiH-CH_2-SiH_2^*$ species. The absence of the SiH_3 stretching modes suggests that the reaction with the silicon in position 3 is not as important as the reaction with the silicon in position 1. This observation has several possible explanations. First, the steric hindrance is probably higher for the SiH_2 group than for the SiH_3 group. Second, the small difference of 2.4 kcal/mol between the computed activation energies of the two reactions cannot be considered meaningful, in view of the approximate description of the infinite surface by means of a finite silicon cluster, the ap-

TABLE III. HREELS experimental peaks and literature based frequencies assignments.

HREELS peaks	Vibrational modes	Corresponding frequency	Mol. or surface species [Ref.]
2950–2980	CH_3 d-str	2982	CH_3SiH_3[a]
	CH_3 s-str	2898	CH_3SiH_3[a]
	CH_2 str	2950	C_2H_4 on Si(100)[b]
2090	SiH_2 str	2095	H_2 on Si(100)[c]
	SiH_2 str	2090	Si_2H_6 on Si(111)[d]
1380	CH_3 d-deform	1403	CH_3SiH_3[a]
	CH_2 bend	1382	CH_2Br_2[e]
1237	CH_3 s-deform	1260	CH_3SiH_3[a]
1030	CH_2 wag	1064	solid 1,4-DSB[f]
880	(SiH_2)n wag	845	Si_2H_6 on Si(111)[d]
	SiH_2 wag	884[g]	
800	(SiH_2)n wag	845	Si_2H_6 on Si(111)[d]
	SiH_2 wag	817[g]	
625	SiH_2 rock	630	Si_2H_6 on Si(111)[d]
	H–SiSi–H bend	621	H_2 on Si(100)[c]

[a]Reference 25.
[b]W. Widdra, C. Huang, G. A. D. Briggs, and W. H. Weinberg, J. Electron. Spectrose. Relat. Phenom. **64**, 129 (1993).
[c]Reference 23.
[d]Reference 22.
[e]T. Shimanouchi, Tables of Molecular Vibrational Frequencies Consolidated Volume I, National Bureau of Standards, 1–160, (1972).
[f]Reference 24.
[g]Calculated for $C_2H_9Si_2^*$ silicon-bonded surface species with strongest IR intensity.

TABLE IV. Comparison between experimental HREEL spectrum and calculated frequencies for different species.

HREELS peaks (cm^{-1})	Vibration modes	$C_2H_9Si_2^*$ 1-Si bonded (cm^{-1})	$C_2H_9Si_2^*$ C bonded (cm^{-1})	$C_2H_9Si_2^*$ 3-Si bonded (cm^{-1})	$CH_3SiH_2^* + CH_2SiH_3^*$ (cm^{-1})	$CH_3-SiH-CH_2-SiH_2^*$ Si bonded (cm^{-1})
2950–3000	CH_3 d-str	3006	⋯	3007, 3000	3012, 3008	3009, 3001
	CH_3 s-str	2970	⋯	2967	2931	2977
	CH_2 str	2928, 2918	2978, 2970 2928, 2920	2925, 2916	2977, 2926	2926, 2922
2090	SiH_3 str	⋯	2149, 2146 2140	2149, 2146 2135	2147, 2145, 2136	⋯
	SiH_2 str	2129 2117, 2106	2137, 2119	⋯	2114, 2109	2120, 2110
	SiH str	⋯	⋯	2104	⋯	2100
1380	CH_3 d-deform	1420	⋯	1418	1418	1418
	CH_2 bend	1365	1365	1364	1363	1373
1237	CH_3 s-deform	1262	⋯	1257	1258	1258
1030	CH_2 wag	1063	1062 1050	1060	1045	1057
	SiH_2 bend	927 914	930	⋯	912	915
880	(SiH_2)n wag	884	908 (SiH_3 s-deform)	911 (SiH_3 s-deform)	908 (SiH_3 s-deform)	911 (SiH_2 bend)
	SiH_2 wag			871 (CH_3 rock)		876 (CH_3 rock)
800	(SiH_2)n wag	817	836	823	859	840
	SiH_2 wag					
625	H–SiSi–H bend	637	630	625	680 (SiH_3 rock)	⋯

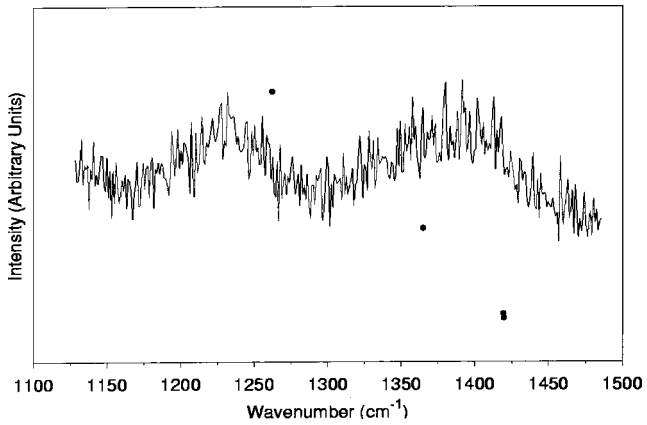

FIG. 5. Close-up of HREEL spectrum of adsorbed 1,3-DSB, 0.5L exposure (solid line) and calculated frequencies and IR intensities for Si-bonded $C_2H_9Si_2$ (●).

proximation on the basis set and the choice of a DFT method that is not as reliable as other computationally more expensive methods such as [QCISD(T)]. Finally, although the SiH_3 stretching mode is absent from the HREELS spectra of chemisorbed DSB, one cannot rule out that a minority of molecules are 3-Si bonded. Indeed, given that the 3-Si bonded $C_2H_9Si_2^*$ has a horizontal geometry with respect to the surface, the dipole scattered intensity from their SiH_3 group would be suppressed due to the HREELS dipole selection rule. (A small impact scattered intensity would still be present, however.)

VI. CONCLUSIONS

Three possible adsorption reactions of 1,3-DSB with Si(100)-(2×1) have been investigated with quantum chemical calculations. They involve the breaking of different bonds in the 1,3-DSB molecule: Silicon–hydrogen, carbon–hydrogen, and silicon–carbon bonds. It was found that the breaking of the silicon–hydrogen bond, leading to the species $C_2H_9Si_2^*$, has the lowest activation energy. The latter can occur by reaction of the silicon in position 1 (11.6 kcal/mol) or by reaction of the silicon in position 3 (9.2 kcal/mol). Experimental data exclude that reaction with silicon in position 3 is dominant. Breaking of the carbon–hydrogen bond and of the silicon–carbon bond are excluded because of the high activation energy (about 30 kcal/mol) required. It is also found that the species $CH_3-SiH-CH_2-SiH_2^*$, corresponding to the horizontal bridging 1,3-DSB, is a very stable species. The formation of this species from the 1-Si bonded $C_2H_9Si_2^*$ has been investigated and activation energy equal to 14.3 kcal/mol has been found. Experimental electron energy loss spectroscopy confirms that the dominant adsorption product is silicon bonded. Agreement between calculation and experiment in the low frequency region also suggests that adsorbed species are likely to be vertically oriented, even if the presence of the horizontal species cannot be ruled out entirely.

On these grounds, we propose that the adsorption path of the 1,3-DSB on Si(100) follows first a reaction between the gas phase molecule and the surface, leading to 1-Si bonded $C_2H_9Si_2^*$ and then, a second reaction between 1-Si bonded $C_2H_9Si_2^*$ and the adjacent silicon dimer to give the silicon bridge bonded $CH_3-SiH-CH_2-SiH_2^*$. Other processes likely take place on the surface during silicon carbide growth but 1,3-DSB adsorption together with hydrogen desorption is expected to be the main rate determining step. For example, Boo *et al.*[6] found an activation energy for the silicon carbide growth equal to 16.4 kcal/mol in conditions where the process is probably adsorption limited (low pressure, i.e., 8.7×10^{-4} Pa). This value is reasonably close to the activation energy calculated in the present work. Of course, one must keep in mind that after the initial step of the growth process, adsorption takes place on the silicon carbide surface rather than on the silicon surface. Work is in progress to develop a detailed kinetic model for silicon carbide film growth using the 1,3-DSB precursor molecule.

ACKNOWLEDGMENTS

The authors gratefully acknowledge the financial support of DARPA MTO and Sandia National Laboratories. The authors also wish to thank Dr. Sudip Mukhopadhyay for the Raman spectrum and Aaron D. Sadow for the IR spectrum. One of the authors (G.V.) acknowledges additional support from the Ministero dell'Universita' e della Ricerca Scientifica e Tecnologica (MURST).

[1] C. H. Carter, Jr. *et al.*, Mater. Sci. Eng., B **61**, 1 (1999).
[2] C. R. Stoldt, M. C. Fritz, C. Carraro, and R. Maboudian, Appl. Phys. Lett. **79**, 347 (2001).
[3] Y. T. Yang, K. L. Ekinci, X. M. H. Huang, L. M. Schiavone, C. Zorman, M. Mehregany, and M. L. Roukes, Appl. Phys. Lett. **78**, 162 (2001).
[4] C. A. Zorman and M. Mehregany, Thin Solid Films **356**, 518 (1999).
[5] T. Kimoto, H. Nishino, W. S. Yoo, and H. Matsunami, J. Appl. Phys. **73**, 726 (1993).
[6] J. H. Boo, S. B. Lee, K. S. Yu, M. M. Sung, and Y. Kim, Surf. Coat. Technol. **131**, 147 (2000).
[7] Y. Ohshita, J. Cryst. Growth **147**, 111 (1995).
[8] S.-C. Park, H. Kang, and S. B. Lee, Surf. Sci. **450**, 117 (2000).
[9] K. Raghavachari, Y. J. Chabal, and L. M. Struck, Chem. Phys. Lett. **252**, 230 (1996).
[10] C. Mui, S. F. Bent, and C. B. Musgrave, J. Phys. Chem. A **104**, 2457 (2000).
[11] R. Konečný and D. J. Doren, Surf. Sci. **417**, 169 (1998).
[12] H. Luo and M. C. Lin, Chem. Phys. Lett. **343**, 219 (2001).
[13] G. Valente, C. Cavallotti, M. Masi, and S. Carra', Proc. Electrochem. Soc., 2001-13 (Fundamental Gas Phase and Surface Chemistry of Vapor-Phase Deposition II), 84 (2001).
[14] A. D. Becke, J. Chem. Phys. **98**, 5648 (1993).
[15] M. J. Frish, G. W. Trucks, H. B. Schlegel *et al.*, GAUSSIAN98, Revision A.6 (Gaussian Inc., Pittsburgh, Pennsylvania, 1998).
[16] An exception occurred for the carbon bonded $C_2H_9Si_2$ [Fig. 1(d)] for which an imaginary frequency was found. Nevertheless, the small absolute value of this frequency (6 cm^{-1}) and the analysis of the associated eigenvector clearly showed that this frequency was associated to the internal rotation of the adsorbed molecule with respect to the cluster around the Si–C bond. Thus, we considered the species stable.

[17] A. P. Scott and L. Radom, J. Phys. Chem. **100**, 16502 (1996).
[18] J. K. Kang and C. B. Musgrave, Phys. Rev. B **64**, 245330 (2001).
[19] A general assessment of the prediction of molecular frequencies in quantum chemical calculations was performed by Scott and Radom (Ref. 17) and Wong (Ref. 20).
[20] M. W. Wong, Chem. Phys. Lett. **256**, 391 (1996).
[21] L. A. Okada, A. C. Dillon, A. W. Ott, and S. M. George, Surf. Sci. **418**, 353 (1998).
[22] R. Imbihl, J. E. Demuth, S. M. Gates, and B. A. Scott, Phys. Rev. B **39**, 5222 (1989).
[23] F. S. Tautz and J. A. Schaefer, J. Appl. Phys. **84**, 6636 (1998).
[24] B. U. Petelenz and H. F. Shurvell, J. Mol. Struct. **64**, 183 (1980).
[25] T. Shimanouchi, Tables of Molecular Vibrational Frequencies Consolidated Volume II, J. Phys. Chem. Ref. Data **6**, 993 (1972).
[26] H. Ibach and D. L. Mills, *Electron Energy Loss Spectroscopy and Surface Vibrations* (Academica, London, UK, 1982).